Single Silicon Neuron Device Enabling Neuronal Oscillation and Stochastic Dynamics

Doohyeok Lim, Kyoungah Cho, and Sangsig Kim

***Abstract*— In this work, we report a fully CMOS-compatible single silicon neuron device, by exploiting interlinked positive and negative feedback loops. The neuron device exhibits the key features of leaky integrate-and-fire functionality and can produce neuronal oscillations that resemble biological oscillations. The stochastic nature and analog input-sensitivity of the feedback switching dynamics are observed in the device. Moreover, the neuronal oscillations of the two-terminal device do not require any power supplied by external bias lines.**

***Index Terms*— Complementary metal-oxide-semiconductor, neuromorphic computing, oscillation, stochastic neuron, leaky integrate-and-fire neuron.**

I. Introduction

WITH the explosion of data generated by the Internet of things (IoT) in the industrial revolution 4.0, classical von Neumann computing has been facing physical and fundamental limitations with respect to data processing [1]. In addition, the continuous scaling of complementary metal–oxide–semiconductor (CMOS) technology is no longer feasible [2]. As a result, new computing paradigms including neuromorphic computing have become necessary to cope with the grand challenges [3]. In biological nervous systems, distributed, parallel, and event-driven computation is efficient, unlike the centralized and sequential computation in von Neumann computing systems [4]. Recently, biomimetic computing systems have been implemented at software levels. However, their hardware is still based on the classical von Neumann architecture [5], [6]. Although CMOS-based neuromorphic circuits have been developed, the complexities of the circuits and a lack of critical dynamics serve as a motivation to exploit the emerging memory device technologies [7]–[10].

In biological cells, interlinked positive and negative feedback loops of chemical reactions generate biological oscillations [11], [12]. Furthermore, the stochasticity in biological neurons plays a key role in providing accuracy in noisy and probabilistic signal processing. Some studies proposed neuron devices to emulate biological systems [13]–[19]. However, spike responses were not from biomimetic feedback dynamics. In addition, their stochastic neuronal functionalities arose from the variations in the fabrication processes [16]. Meanwhile, some simple relaxation oscillator circuits are well known for their spiking capabilities [20]–[22]; external bias voltages are indispensable for three-terminal structures to operate these circuits. Despite some recent works on other device stacks that can also mimick the performance of a neuron, the NbO_2-based material stacks are still challenging for practical devices and systems [23], [24].

Thyristor-random access memories (T-RAMs), which employ p-n-p-n structures, provide positive feedback loop [25]–[27]. Nevertheless, T-RAMs have also three-terminal structures which are not suitable for artificial neuron. In this study, we introduce a single two-terminal silicon neuron device with oscillatory and stochastic neuronal dynamics by using interlinked positive and negative feedback loops.

II. Experimental

The single silicon neuron device was fabricated from a p-type (100)-oriented SOI wafer with resistivity 18–22 $\Omega\cdot$cm, using fully CMOS processes (Fig. 1). The n-doped regions were formed by a conventional n-well process with a doping concentration of $\sim 10^{17}$ cm^{-3}. The doping concentration of the p-doped regions was $\sim 10^{18}$ cm^{-3}. A poly-Si gate with a physical length of 2.5 μm was formed by low-pressure chemical vapor deposition onto the SiO_2 gate oxide layer. Also, heavily doped p^+ drain and n^+ source regions ($\sim 10^{20}$ cm^{-3}) were created by masked ion implantations. Conventional Ti/TiN/Al/TiN metal stacks were used to contact the drain, source, and gate regions.

III. Results and Discussion

The single silicon neuron device consists of a p^+–n–p–n^+ diode with connected drain and gate terminals, resistors (R_1 and R_2), and a parasitic capacitance from the output node V_{out} to the ground (Fig. 2(a)). The resistance R_1 sets a compliance current to generate interlinked positive and negative feedback loops. The diode generates the positive and negative feedback loops. And the resistance R_2 converts the signals from interlinked positive and negative feedback loops into voltage spikes. The two-terminal design allows the device to function as a threshold switch for neuron oscillations [28].

The measured $I-V$ characteristics are shown in Fig. 2(b). When the voltage (V_{DD}) is swept from 0 to 3 V in medium mode (HP 4155C), an abrupt increase in current, which corresponds to the latch-up state, is observed at a certain

Manuscript received February 8, 2021; revised February 25, 2021; accepted March 2, 2021. Date of publication March 4, 2021; date of current version April 26, 2021. This work was supported in part by the Ministry of Trade, Industry and Energy (MOTIE) under Grant 10067791, in part by the Korea Semiconductor Research Consortium (KSRC) Support Program for the development of future semiconductor devices, in part by the National Research Foundation of Korea (NRF) Grant by the Korean Government through the Ministry of Science and ICT (MSIT) under Grant 2020R1A2C3004538, in part by the Brain Korea 21 Plus Project in 2021, and in part by the Korea University Grant. The review of this letter was arranged by Editor B. Govoreanu. *(Corresponding author: Sangsig Kim.)*

The authors are with the School of Electrical Engineering, Korea University, Seoul 02841, South Korea (e-mail: sangsig@korea.ac.kr).

Color versions of one or more figures in this letter are available at https://doi.org/10.1109/LED.2021.3063954.

Digital Object Identifier 10.1109/LED.2021.3063954

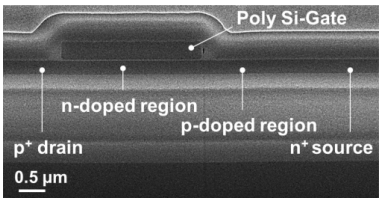

Fig. 1. Scanning electron microscope image of the single silicon neuron device.

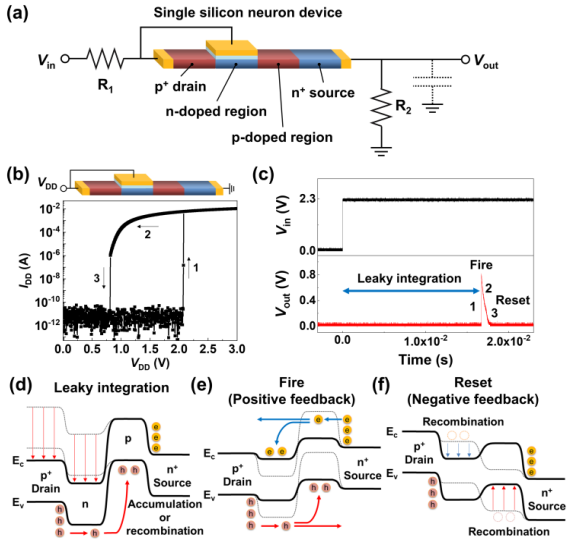

Fig. 2. Single silicon neuron device implementation. (a) Diagram of neuron device comprising the single silicon neuron device, two resistors, and a parasitic capacitor. The resistances R_1 and R_2 are 10 MΩ and 1 MΩ, respectively. (b) $I-V$ characteristics of the single neuron device. (c) Spike response of the neuron device provided by positive and negative feedback loops. Energy-band diagrams of the single silicon neuron device in its (d) leaky integration state, (e) firing state, and (f) reset state.

voltage ($V_{\text{latch-up}}$) because of the generation of a positive feedback loop. During the reverse bias sweep, the formation of a negative feedback loop triggers an abrupt decrease in current at a certain voltage ($V_{\text{latch-down}}$), i.e., the latch-down state. These interlinked positive and negative feedback loops, which correspond to the mutual interactions between the latch-up and latch-down states, generate neuronal oscillations.

The oscillatory neuronal behaviors were characterized, as shown in Fig. 2(c). After the integration of a certain period of input voltage (V_{in}), the neuron device generated an output signal (i.e., the device fired) when a membrane potential crossed the firing threshold. The firing event was enabled by the positive feedback loop (Fig. 2, (b) and (c), curve 1). As the device reached the latch-up state, because of the firing event, the voltage across the resistors increased suddenly. As V_{in} was constant, the immediate voltage across the device decreased, driving the device back into the latch-down state. After reaching the firing threshold, the device was automatically reset to the initial state, enabled by the negative feedback loop (Fig. 2, (b) and (c), curves 2 and 3).

Energy band diagrams illustrate the leaky integrate-and-fire dynamics (Fig. 2(d) to 2(f)). The n- and p-doped regions, which act as the membranes, create potential wells for charge-carrier accumulation, thereby allowing the device to integrate presynaptic signals. In addition, the recombination of the accumulated charge carriers in the potential wells allows the integrated input signal to decay, which corresponds to the leaky membrane potential. When input voltages are applied to the neuron devices, holes can accumulate at the potential well of the p-doped region or recombine if there is no input (Fig. 2(d)), i.e., leaky integration. During the leaky integration, the accumulation of holes lowers the height of the potential barrier formed at the p-doped region, thereby allowing the electrons in the n^+ source to accumulate at the n-doped region and flow toward the p^+ drain. The accumulation of electrons also encourages the injection of more holes.

The mutual interaction between the potential barriers and charge carriers produces the positive feedback loop, which leads to the diode in the latch-up state. If the threshold is reached by the accumulation of the charge carriers in the potential wells, the positive feedback loop is activated, and the neuron fires (Fig. 2(e)). Until the neuron fires, the voltage across the device in the latch-up state decreases because of the resistors, thus triggering the negative feedback loop. This drives the device back into the latch-down state after an effective refractory period (Figs. 2, (b) and (c), curve 2), thereby resetting the initial threshold (Fig. 2(f)).

The neuron spiking behaviors with oscillatory neuronal dynamics were investigated by applying diverse input signals (Fig. 3). When V_{in} was below 2.3 V, no oscillations were generated. The conditions for oscillation had to be satisfied:

$$\frac{V_{\text{in}} \times R_{\text{latch-down}}}{R_{\text{latch-down}} + R_1 + R_2} \geq V_{\text{latch-up}}, \tag{1}$$

$$\frac{V_{\text{in}} \times R_{\text{latch-up}}}{R_{\text{latch-up}} + R_1 + R_2} \leq V_{\text{latch-down}}. \tag{2}$$

Here, $R_{\text{latch-down}}$ is the resistance of the single silicon neuron device in the latch-down state and $R_{\text{latch-up}}$ is the resistance of the device in the latch-up state. When a pulse amplitude of 2.3 V is fed into the input, neuronal oscillations with integrate-and-fire functionalities are observed (Fig. 3(a)). The integrate-and-fire dynamics were enabled by the generation of the positive feedback loop in the device, which is similar to the ion channels in biological neurons. Moreover, the device was automatically reset to the initial state after the firing event because the output spike triggered the negative feedback loop. The positive and negative feedback loops could create multiple consecutive spike events, i.e., neuronal oscillations. The number of spike events within a defined time interval can be tuned by adjusting the input amplitude. As V_{in} changed from 2.3 to 3.1 V, the tuning linearity of the spike events was observed (Fig. 3(b)). The modulation of the input signals allows a tunable integration time in the neuronal oscillations.

The leaky integrate-and-fire functionality was demonstrated by applying consecutive pulses to the input node (Fig. 3(c)). An input voltage of 0 V between consecutive pulses resulted in the recombination of the accumulated charge carriers in the potential wells, enabling leaky integration. After the arrival of five pulses into the neuron device, the membrane potential reached the threshold and the neuron device fired. The spike response of the analog or mixed signals in the artificial neuron was one of the most important neuronal functionalities for analog computation in neural networks [29]. Analog tuning in the artificial neurons is implemented by the modulation of

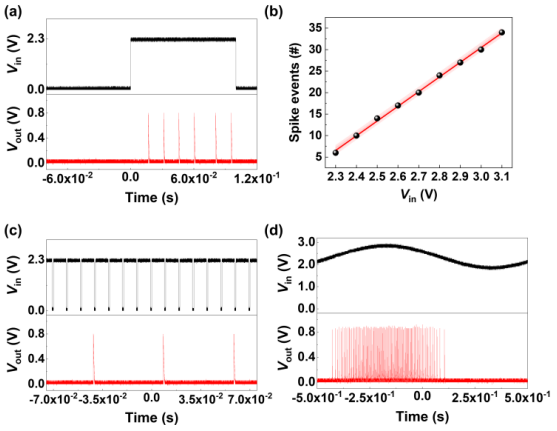

Fig. 3. Neuron spiking behaviors in single silicon neuron devices. (a) Spike response of integrate-and-fire neuron to constant DC input. (b) Number of spike events as a function of the input voltage amplitude with a pulse duration of 100 ms. (c) Leaky integrate-and-fire functionality of a single neuron device. (d) Analog input-sensitive oscillations in one complete cycle of a sinusoidal waveform.

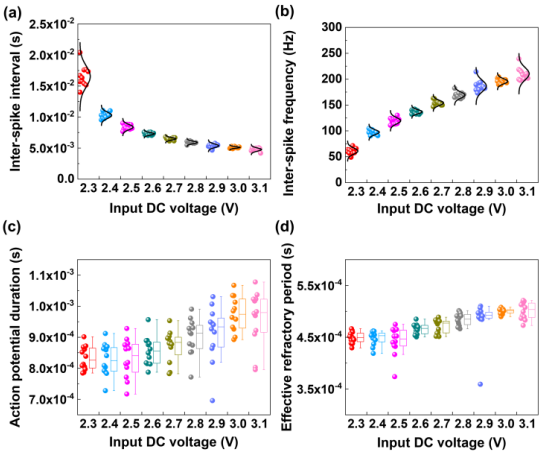

Fig. 4. Stochastic spike characteristics of single silicon neuron device. (a) Distribution of consecutive inter-spike intervals in a neuron device. Spike trains are excited by various input DC voltages. (b) Frequency responses of the leaky integrate-and-fire neuron to different input DC voltage values. (c) Variability of action potential duration as a function of the value of the input stimulus. (d) Deviation of effective refractory period in the single silicon neuron with input DC bias in the range 2.3–3.1 V.

the neuronal oscillation frequency when a sinusoidal waveform is applied to the input node (Fig. 3(d)). Although the sinusoidal input signals exceeded the stimulation threshold, the amplitudes of the individual spikes were nearly constant. The neuronal oscillatory dynamics by analog or mixed signals allowed our device to implement biologically plausible leaky integrate-and-fire neurons.

The single two-terminal silicon neuron device exhibits a lower energy value of ∼719 pJ/spike and occupies a smaller area, compared to CMOS-based neurons devices that use complex circuits including source followers, inverters, reset circuits, and current-to-voltage converters [34]–[37]. The two-terminal configuration in our device enables the leaky integrate-and-fire functions without external applied voltages, whereas three-terminal configuration in CMOS-based neurons devices does not. As the resistors cannot affect the whole device scalability, it is expected that the scaled device allows sub-1-V operation and sub-pJ energy consumption.

The neuronal activity in biological systems exhibited complex stochastic behaviors owing to the noisy, irregular, and unreliable molecular mechanisms [30]–[32]. Stochastic operation plays a key role in complex computational tasks in neuronal networks; an example would be the Bayesian inference, performed by stochastic neuronal populations [33]. The capability of the spike response from the analog inputs to the device (Fig. 3(d)) enabled stochastic firing responses for developed neuronal networks. In addition, stochastic feedback switching dynamics were inherent in the device because of the accumulation and recombination of charge carriers in the potential wells by the Shockley–Read–Hall generation and recombination or band-to-band tunneling, which are probabilistic processes. Thus, the native physics of the single silicon neuron device could realize stochastic behaviors for neuronal computation.

The inherent stochasticity of the single silicon neuron device led to a distribution of inter-spike intervals, defined as the time difference between consecutive spikes in multiple leaky integrate-and-fire cycles (Fig. 4(a)). Our device shows approximately symmetrical distributions of inter-spike intervals. Nevertheless, as the amplitude of the input DC voltage varied from 2.3 to 3.1 V, the inter-spike intervals around the mean response of consecutive spikes decreased. Variations were also observed in the frequency responses of the leaky integrate-and-fire neurons (Fig. 4(b)). While the mean firing rate of the consecutive spikes could be modulated from 61.0 to 210.5 Hz by increasing the magnitude of the input signal from 2.3 to 3.1 V, the consistency of the spike amplitudes and stochasticity of the frequency responses were retained. Fig. 4(c) shows that the variability of the action potential duration was not dependent on the magnitude of the input stimulus. It indicates that the interlinked positive and negative feedback loops in the device bore a resemblance to the feedback mechanism in biological cells. The effective refractory period over the range of the input signal exhibited irregularity and skewed distribution, as shown in Fig. 4(d).

IV. Conclusion

In summary, inspired by the interlinked positive and negative feedback loops in biological cells, the leaky integrate-and-fire functionalities with oscillatory and stochastic dynamics were demonstrated in a single silicon neuron device. Moreover, our two-terminal device produces neuronal oscillations without power supplied by external bias lines. The capability of analog input-sensitive neuronal behaviors with oscillatory and stochastic dynamics can open up possibilities to revolutionize the entire neuromorphic hardware technology.

References

[1] P. A. Merolla, J. V. Arthur, R. Alvarez-Icaza, A. S. Cassidy, J. Sawada, F. Akopyan, B. L. Jackson, N. Imam, C. Guo, Y. Nakamura, B. Brezzo, I. Vo, S. K. Esser, R. Appuswamy, B. Taba, A. Amir, M. D. Flickner, W. P. Risk, R. Manohar, and D. S. Modha, "A million spiking-neuron integrated circuit with a scalable communication network and interface," *Science*, vol. 345, no. 6197, pp. 668–673, 2014, doi: 10.1126/science.1254642.

[2] M. M. Waldrop, "The chips are down for Moore's law," *Nature*, vol. 530, no. 7589, p. 144, 2016.

[3] Beyond CMOS. *International Roadmap for Devices and Systems*. Accessed: Jan. 2020. [Online]. Available: https://irds.ieee.org/editions/2020/beyond-cmos

[4] S. Furber, "Large-scale neuromorphic computing systems," *J. Neural Eng.*, vol. 13, no. 5, Oct. 2016, Art. no. 051001, doi: 10.1088/1741-2560/13/5/051001.

[5] D. Silver, J. Schrittwieser, K. Simonyan, I. Antonoglou, A. Huang, A. Guez, T. Hubert, L. Baker, M. Lai, A. Bolton, Y. Chen, T. Lillicrap, F. Hui, L. Sifre, G. van den Driessche, T. Graepel, and D. Hassabis, "Mastering the game of go without human knowledge," *Nature*, vol. 550, no. 7676, pp. 354–359, Oct. 2017, doi: 10.1038/nature24270.

[6] Y. LeCun, Y. Bengio, and G. Hinton, "Deep learning," *Nature*, vol. 521, no. 7553, pp. 436–444, May 2015, doi: 10.1038/nature14539.

[7] S. Ambrogio, P. Narayanan, H. Tsai, R. M. Shelby, I. Boybat, C. Di Nolfo, S. Sidler, M. Giordano, M. Bodini, N. C. P. Farinha, B. Killeen, C. Cheng, Y. Jaoudi, and G. W. Burr, "Equivalent-accuracy accelerated neural-network training using analogue memory," *Nature*, vol. 558, no. 7708, pp. 60–67, Jun. 2018, doi: 10.1038/s41586-018-0180-5.

[8] M. Prezioso, F. Merrikh-Bayat, B. D. Hoskins, G. C. Adam, K. K. Likharev, and D. B. Strukov, "Training and operation of an integrated neuromorphic network based on metal-oxide memristors," *Nature*, vol. 521, no. 7550, pp. 61–64, May 2015, doi: 10.1038/nature14441.

[9] Z. Wang, S. Joshi, S. E. Savel'ev, H. Jiang, R. Midya, P. Lin, M. Hu, N. Ge, J. P. Strachan, Z. Li, Q. Wu, M. Barnell, G.-L. Li, H. L. Xin, R. S. Williams, Q. Xia, and J. J. Yang, "Memristors with diffusive dynamics as synaptic emulators for neuromorphic computing," *Nature Mater.*, vol. 16, no. 1, pp. 101–108, Jan. 2017, doi: 10.1038/nmat4756.

[10] M. Jerry, P.-Y. Chen, J. Zhang, P. Sharma, K. Ni, S. Yu, and S. Datta, "Ferroelectric FET analog synapse for acceleration of deep neural network training," in *IEDM Tech. Dig.*, Dec. 2017, pp. 6.2.1–6.2.4, doi: 10.1109/IEDM.2017.8268338.

[11] T. Y.-C. Tsai, Y. S. Choi, W. Ma, J. R. Pomerening, C. Tang, and J. E. Ferrell, "Robust, tunable biological oscillations from interlinked positive and negative feedback loops," *Science*, vol. 321, no. 5885, pp. 126–129, Jul. 2008, doi: 10.1126/science.1156951.

[12] O. Brandman and T. Meyer, "Feedback loops shape cellular signals in space and time," *Science*, vol. 322, no. 5900, pp. 390–395, Oct. 2008, doi: 10.1126/science.1160617.

[13] M. D. Pickett, G. Medeiros-Ribeiro, and R. S. Williams, "A scalable neuristor built with Mott memristors," *Nature Mater.*, vol. 12, no. 2, pp. 114–117, Feb. 2013, doi: 10.1038/nmat3510.

[14] P. Stoliar, J. Tranchant, B. Corraze, E. Janod, M.-P. Besland, F. Tesler, M. Rozenberg, and L. Cario, "A leaky-integrate-and-fire neuron analog realized with a Mott insulator," *Adv. Funct. Mater.*, vol. 27, no. 11, Mar. 2017, Art. no. 1604740, doi: 10.1002/adfm.201604740.

[15] I. Gupta, A. Serb, A. Khiat, R. Zeitler, S. Vassanelli, and T. Prodromakis, "Real-time encoding and compression of neuronal spikes by metal-oxide memristors," *Nature Commun.*, vol. 7, no. 1, Nov. 2016, Art. no. 012805, doi: 10.1038/ncomms12805.

[16] T. Tuma, A. Pantazi, M. Le Gallo, A. Sebastian, and E. Eleftheriou, "Stochastic phase-change neurons," *Nature Nanotechnol.*, vol. 11, no. 8, pp. 693–699, Aug. 2016, doi: 10.1038/nnano.2016.70.

[17] W. Yi, K. K. Tsang, S. K. Lam, X. Bai, J. A. Crowell, and E. A. Flores, "Biological plausibility and stochasticity in scalable VO_2 active memristor neurons," *Nature Commun.*, vol. 9, no. 1, p. 4661, Dec. 2018, doi: 10.1038/s41467-018-07052-w.

[18] Z. Wang, M. Rao, J.-W. Han, J. Zhang, P. Lin, Y. Li, C. Li, W. Song, S. Asapu, R. Midya, Y. Zhuo, H. Jiang, J. H. Yoon, N. K. Upadhyay, S. Joshi, M. Hu, J. P. Strachan, M. Barnell, Q. Wu, H. Wu, Q. Qiu, R. S. Williams, Q. Xia, and J. J. Yang, "Capacitive neural network with neuro-transistors," *Nature Commun.*, vol. 9, no. 1, p. 3208, Dec. 2018, doi: 10.1038/s41467-018-05677-5.

[19] Z. Wang, S. Joshi, S. Savel'ev, W. Song, R. Midya, Y. Li, M. Rao, P. Yan, S. Asapu, Y. Zhuo, H. Jiang, P. Lin, C. Li, J. H. Yoon, N. K. Upadhyay, J. Zhang, M. Hu, J. P. Strachan, M. Barnell, Q. Wu, H. Wu, R. S. Williams, Q. Xia, and J. J. Yang, "Fully memristive neural networks for pattern classification with unsupervised learning," *Nature Electron.*, vol. 1, no. 2, pp. 137–145, Feb. 2018, doi: 10.1038/s41928-018-0023-2.

[20] K. Crisp, "Models for spiking neurons: Integrate-and-fire units and relaxation oscillators," *J. Undergraduate Neurosci. Educ.*, vol. 17, no. 2, pp. E7–E12, 2019. [Online]. Available: https://pubmed.ncbi.nlm.nih.gov/31360134 and https://www.ncbi.nlm.nih.gov/pmc/articles/PMC6650253/

[21] W. J. Askew, "Unijunction transistor artificial neuron," U.S. Patent 3 691 400, Sep. 12, 1972.

[22] M. Nurujjaman, P. S. Bhattacharya, A. N. S. Iyengar, and S. Sarkar, "Coherence resonance in a unijunction transistor relaxation oscillator," *Phys. Rev. E, Stat. Phys. Plasmas Fluids Relat. Interdiscip. Top.*, vol. 80, no. 1, Jul. 2009, Art. no. 015201, doi: 10.1103/PhysRevE.80.015201.

[23] S. Kumar, R. S. Williams, and Z. Wang, "Third-order nanocircuit elements for neuromorphic engineering," *Nature*, vol. 585, no. 7826, pp. 518–523, Sep. 2020, doi: 10.1038/s41586-020-2735-5.

[24] S. Kumar, J. P. Strachan, and R. S. Williams, "Chaotic dynamics in nanoscale NbO_2 Mott memristors for analogue computing," *Nature*, vol. 548, no. 7667, pp. 318–321, Aug. 2017, doi: 10.1038/nature23307.

[25] D. Resnati, C. M. Compagnoni, H. Mulaosmanovic, N. Castellani, G. Carnevale, P. Fantini, D. Ventrice, A. L. Lacaita, A. S. Spinelli, and A. Benvenuti, "Modeling of dynamic operation of T-RAM cells," *IEEE Trans. Electron Devices*, vol. 62, no. 6, pp. 1905–1911, Jun. 2015, doi: 10.1109/TED.2015.2421556.

[26] H. Mulaosmanovic, G. M. Paolucci, C. M. Compagnoni, N. Castellani, G. Carnevale, P. Fantini, D. Ventrice, A. L. Lacaita, A. S. Spinelli, and A. Benvenuti, "Working principles of a DRAM cell based on gated-thyristor bistability," *IEEE Electron Device Lett.*, vol. 35, no. 9, pp. 921–923, Sep. 2014, doi: 10.1109/LED.2014.2336674.

[27] D. Lim, J. Son, K. Cho, and S. Kim, "Quasi-nonvolatile silicon memory device," *Adv. Mater. Technol.*, vol. 5, no. 12, Dec. 2020, Art. no. 2000915, doi: 10.1002/admt.202000915.

[28] P. Wang, A. I. Khan, and S. Yu, "Cryogenic behavior of NbO_2 based threshold switching devices as oscillation neurons," *Appl. Phys. Lett.*, vol. 116, no. 16, Apr. 2020, Art. no. 162108, doi: 10.1063/5.0006467.

[29] M. Hu, C. E. Graves, C. Li, Y. Li, N. Ge, E. Montgomery, N. Davila, H. Jiang, R. S. Williams, J. J. Yang, Q. Xia, and J. P. Strachan, "Memristor-based analog computation and neural network classification with a dot product engine," *Adv. Mater.*, vol. 30, no. 9, Mar. 2018, Art. no. 1705914, doi: 10.1002/adma.201705914.

[30] R. B. Stein, E. R. Gossen, and K. E. Jones, "Neuronal variability: Noise or part of the signal?" *Nature Rev. Neurosci.*, vol. 6, no. 5, pp. 389–397, May 2005, doi: 10.1038/nrn1668.

[31] Y. Yarom and J. Hounsgaard, "Voltage fluctuations in neurons: Signal or noise?" *Physiol. Rev.*, vol. 91, no. 3, pp. 917–929, 2011, doi: 10.1152/physrev.00019.2010.

[32] E. T. Rolls and G. Deco, *The Noisy Brain: Stochastic Dynamics as a Principle of Brain Function*. London, U.K.: Oxford Univ. Press, 2010.

[33] W. J. Ma, J. M. Beck, P. E. Latham, and A. Pouget, "Bayesian inference with probabilistic population codes," *Nature Neurosci.*, vol. 9, no. 11, pp. 1432–1438, Nov. 2006, doi: 10.1038/nn1790.

[34] G. Indiveri, E. Chicca, and R. Douglas, "A VLSI array of low-power spiking neurons and bistable synapses with spike-timing dependent plasticity," *IEEE Trans. Neural Netw.*, vol. 17, no. 1, pp. 211–221, Jan. 2006, doi: 10.1109/TNN.2005.860850.

[35] J.-K. Han, M. Seo, J.-M. Yu, Y.-J. Suh, and Y.-K. Choi, "A single transistor neuron with independently accessed double-gate for excitatory-inhibitory function and tunable firing threshold voltage," *IEEE Electron Device Lett.*, vol. 41, no. 8, pp. 1157–1160, Aug. 2020, doi: 10.1109/LED.2020.3001953.

[36] Z. Wang, B. Crafton, J. Gomez, R. Xu, A. Luo, Z. Krivokapic, L. Martin, S. Datta, A. Raychowdhury, and A. I. Khan, "Experimental demonstration of ferroelectric spiking neurons for unsupervised clustering," in *IEDM Tech. Dig.*, Dec. 2018, pp. 13.3.1–13.3.4, doi: 10.1109/IEDM.2018.8614586.

[37] S. Dutta, V. Kumar, A. Shukla, N. R. Mohapatra, and U. Ganguly, "Leaky integrate and fire neuron by charge-discharge dynamics in floating-body MOSFET," *Sci. Rep.*, vol. 7, no. 1, p. 8257, Dec. 2017, doi: 10.1038/s41598-017-07418-y.